Determination of Optimal Modules Number in Photovoltaic Strings for Inverter Power Maximization

Ljupco Trpezanovski[1], Dimitar Dimitrov[2]

Abstract – **In this paper is presented a way for determination the optimal number of photovoltaic (PV) modules connected in a string. The aim for optimal number of modules determination is to obtain the optimal working voltage on inverter DC side and activate the device for Maximal Power Point Tracker – MPPT. The calculations are performed according the PV module and inverter data for Standard Test Conditions and defined specific working scenarios. After that, a way for determination of optimal number of strings connected to the inverter is shown. The calculations are performed under condition to gain the maximum active power from the inverter in all possible working scenarios (working states of the inverter with activated MPPT device). To avoid the inverter damage, during the calculations the inverter limiting working performances are taken into account. The proposed methodology in this paper is practically applied on PV modules from Yingli Solar Company of China and inverter from the SMA Company of Germany.**

Keywords – **Photovoltaic modules, DC/AC inverter, maximum active power, photovoltaic power plants.**

I. INTRODUCTION

The total energy from the solar radiation which yearly reaches the Earth is about 10^{18} kWh/year. This energy is 60.000 times greater then the yearly consumed electricity and 25 times greater from the all fossil energy potentials on the Earth. Because of the energy losses in the atmosphere (absorption and reflection) the average daily energy reaches the Earth surface is about 5,52 kWh/m^2 [1]. For the specific location on the Earth the exact value of solar radiation will depend of a latitude, longitude and elevation of the location, season (position of the Sun over horizon), temperature, presence of: fog, clouds, pollution, wind etc. Consequently, it is obvious that the Sun is the biggest and main source of renewable energy. The geographical position and a climate in the Republic of Macedonia offer very good perspective for solar energy utilization. The average daily radiation per year is between 3,4 kWh/m^2 in the north part of the country (Skopje) and 4,2 kWh/m^2 in the south-west part (Bitola). Total solar radiation per year varies from minimum 1250 kWh/m^2 in the north to maximum 1530 kWh/m^2 in the south-west part of the country. Therefore, the yearly average solar radiation is 1390 kWh/m^{2}year [2]. In the Study for renewable sources of energy in the Republic of Macedonia [2] and Strategy for energy sector development in the Republic of Macedonia in the period 2008-2020 [3] (published by the Macedonian Academy of Sciences and Arts) is predicted construction of 10 to 30 MWp photovoltaic power plants (PVP). These PVP will produce electricity from 14 to 60 GWh/year.

Solar energy transformation in the electricity is directly performed in the photovoltaic (PV) solar cells grouped in solar modules. For more electrical power, the modules are connecting in serial and form a string. More strings can be connected in parallel. The electricity produced in PV modules is on direct current (DC). The electricity conversion from DC to alternative current (AC) is performing in the inverters. With the set of PV modules (connected in strings) and inverter(s) altogether connected in proper way, the PVP are constructed. The purpose of PVP is production of electricity directly with solar energy transformation. The produced electricity can be used individually from separated consumers (Off-Grid) or be injected into a power distribution system (On-Grid).

During the PVP design and construction it is necessary to take into account a way for strings forming and their connection to the inverter(s). These procedures are required because the aim is to get maximum produced electricity from the solar radiated energy on the PV modules surface in combination with inverter(s) optimal working performances.

In this paper from theoretical and practical aspect on the real case of applied PV modules and inverter a way for determination of optimal photovoltaic modules number in a string and optimal strings number connected into inverter for active power maximization is presented.

In the section II the main characteristics for photovoltaic modules and inverters necessary for proposed calculations are given. The calculations for certain types of PV module and inverter are shown in section III. The conclusions are drawn in the section IV.

II. PHOTOVOLTAIC MODULE AND INVERTER CHARACTERISTICS

The determination of the optimal PV modules number in a string depends of the module characteristics and optimal working performances of the inverter in which the string(s) is/are connected. The theoretical calculations are practically applied on the PV module Yingli Solar type YL235P-29b with power output of 235 Wp [4].

The current-voltage (I-V) diagram of this type of PV modules is given on Fig. 1. On this figure can be seen that for different intensity of solar radiation exists only one point on the I-V diagram for which the product $V \cdot I$ has maximal value. More exactly, for each curve exists only one working point (named Maximal Power Point – MPP) in which the PV

[1]Ljupco Trpezanovski is with the Faculty of Technical Sciences at University St. Kliment Ohridski, Bitola, Makedonska Falanga 33, 7000 Bitola, Republic of Macedonia,
E-mail: ljupco.trpezanovski@gmail.com

[2]Dimitar Dimitrov is with the Faculty of Electrical Engineering and Information Technologies at University Ss. Ciril and Methodius, Skopje, Rugjer Boshkovik bb, 1000 Skopje, Republic of Macedonia.

module voltage is V_{MPP} and flows current I_{MPP} with production of maximal power $P_{MPP} = V_{MPP} \cdot I_{MPP}$.

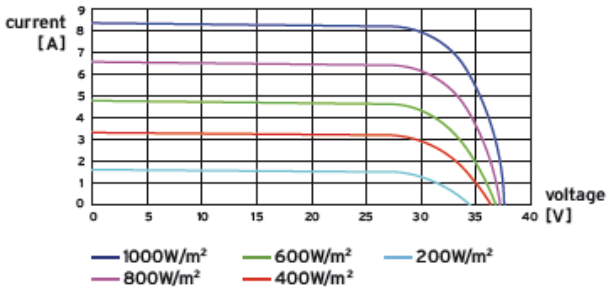

Fig. 1. *I-V* diagram for PV module type YL235P-29b.

In case for Standard Test Conditions – STC (radiation 1000 W/m^2, air mass coefficient AM=1,5 and temperature T=25^{0}C) applied on PV module YL235P-29b, the *I-V* and $P = f(I,V)$ diagrams are shown on Fig. 2. The function $P = f(I,V)$ shows how PV module output power depends from module voltage and current. Open circuit voltage, signed as V_{OC} is a voltage on not connected plugs of the radiated PV module on STC. A short circuit current, signed as I_{SC} is current through the PV module output when the plugs are short connected.

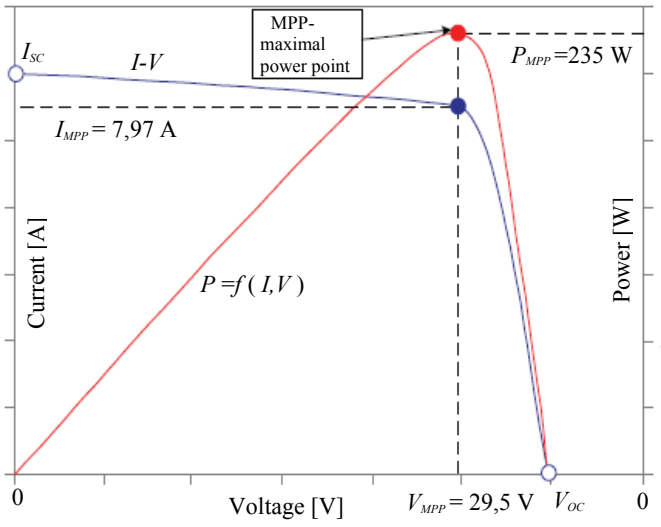

Fig. 2. *I-V* and $P = f(I,V)$ diagrams for module YL235P-29b.

The main aim for calculation of optimal PV modules number in a string is to gain maximal active power from the string. In other words, obtained string voltage should be in such interval that with application of Maximum Power Point Tracker (MPPT) device built in the inverter provides inverter working voltage $U_{MPPT} = V_{MPP}$ and current through inverter I_{MPP}. The other electrical and thermal characteristics for the PV module type YL235P-29b for STC conditions are given in Table I.

The electricity produced by a string or group of strings connected in parallel is on DC voltage. It is necessary to convert the electricity from DC to AC voltage if PVP will be connected on a grid. For that purpose group of strings is connected on DC/AC inverter(s).

TABLE I
ELECTRICAL AND THERMAL PV MODULE CHARACTERISTICS [4].

PV module type	**YL235P-29b**	
Power output	[W]	235,0
Power output tolerance	[%]	± 3
Module efficiency	[%]	14,4
Voltage at P_{max}, V_{MPP}	[V]	29,5
Current at P_{max}, I_{MPP}	[A]	7,97
Open circuit voltage V_{OC}	[V]	37,0
Short circuit current I_{SC}	[A]	8,54
Nominal operation Cell Temp. NOCT	[^{0}C]	46 ±2
Temperature coefficient ΔI_{SC}	[1/^{0}C]	+ 0,0006
Temperature coefficient ΔV_{OC}	[1/^{0}C]	– 0,0037
Temperature coefficient ΔV_{MPP}	[1/^{0}C]	– 0,0045

This type of inverter converts the electricity from DC voltage on AC voltage with minimal losses of electricity. If in the inverter has built in the MPPT device in certain intensity of solar radiation the group of strings will delivered maximum DC power to the inverter. For practical analysis in this paper, inverter type SMA SMC 11000TL [5] is taken in consideration. This inverter is from German producer SMA Solar Technology AG and has very good characteristics. The efficiency curves [5], for different AC powers P_{AC} (on the output) and different DC voltages V_{DC} (on the DC input) are shown on Fig 3.

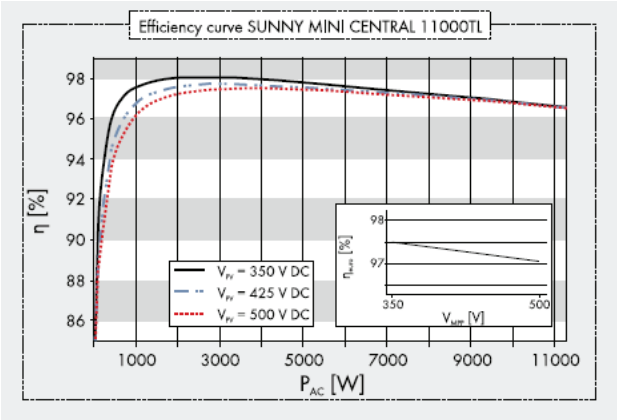

Fig. 3. SMC 11000TL inverter efficiency η[%] curves [5].

All technical data for the inverter necessary for determination of optimal PV modules number in a string and optimal number of strings connected into inverter DC input are given in Table II. It should be taken into account that practically only 5 strings can be connected to the inverter DC input with one MPPT device.

TABLE II
TECHNICAL DATA FOR INVERTER TYPE SMC 11000TL [5].

Input (DC)		
Maximum DC power	[W]	11.400
Maximum DC voltage	[V]	700
MPP voltage range	[V]	333 − 500
DC nominal voltage	[V]	350
Minimum DC voltage / start voltage	[V]	333/400
Maximum input current / per string	[A]	34/34
Number of MPPT / strings per MPPT	No	1/5
Output (AC)		
AC nominal power (230 V, 50 Hz)	[W]	11.000
Nominal AC voltage range	[V]	180 − 260
AC grid frequency range	[Hz]	50 - 60±4,5
Maximum output current	[A]	48
Power factor (cosφ)	[p.u.]	1
Efficiency / Euro-eta	[%]	98,0 / 97,5

III. DETERMINATION OF OPTIMAL NUMBER OF PV MODULES IN A STRING AND STRINGS IN INVERTER

For certain intensity of solar radiation the string or group of strings (PV generator) will delivered maximum DC power to the inverter if it's MPPT device is activated. According to the technical data of the inverter SMA SMC 11000TL (Table II), the MPPT device will be active if inverter input DC voltage U_{PV} is between 333 and 500 V, or:

$$U_{MPPT,\min} = 333\,V \le U_{PV} \le 500\,V = U_{MPPT,\max}. \quad (1)$$

This voltage range should be achieved during the long time of PV generator operation. According to the recommendations of inverter producer it is necessary to check the PV generator voltage in the Maximal Power Point V_{MPP} for PV cells temperature of 15 ^{0}C and 70 ^{0}C. The V_{MPP} for a PV module on temperature T can be calculated by Eq. (2), [6]:

$$V_{MPP,T} = V_{MPP,STC}\left[1 + \frac{\Delta V_{MPP}}{100}(T - 25)\right], \quad (2)$$

where ΔV_{MPP} is temperature coefficient for voltage changing in MPP and $V_{MPP,STC}$ is PV module voltage in MPP for STC. These values for PV module type YL235P-29b are: $\Delta V_{MPP} = -0{,}45\,\%/^0\text{C}$ and $V_{MPP,STC} = 29{,}5$ V. Applying the Eq. (2) for the proposed PV module obtained values are: for cells temperature T=15 ^{0}C the MPP voltage is $V_{MPP,15} = 30{,}8$ V and for T=70 ^{0}C $V_{MPP,70} = 23{,}5$ V.

Taking into account recommendations and also parameters of inverter and PV module the permitted number of PV modules in a string can take values from $n_{\min}$ to $n_{\max}$. For the proposed inverter and PV module these numbers are obtained through Eqs. (3) and (4) taken from [6]:

$$n_{\min} = \frac{U_{MPPT,\min}}{V_{MPP,70}} = \frac{333}{23{,}5} = 14{,}17 \Rightarrow n_{\min} = 15 \text{ modules/string} \quad (3)$$

$$n_{\max} = \frac{U_{MPPT,\max}}{V_{MPP,15}} = \frac{500}{30{,}8} = 16{,}23 \Rightarrow n_{\max} = 16 \text{ modules/string.} \quad (4)$$

Inverter producers proposed maximal value for input DC voltage. For inverter SMC 11000TL this voltage is 700 V. During the calculation process for PV module number in a string it is necessary to check if string voltage exceeds maximal input DC voltage. For this check the cells temperature should be T=−10 ^{0}C. The worst case for voltage increasing is when the PV string (or PV generator) is working in open circuit. If the cells temperature is different than that in STC, the open circuit voltage can be calculated with Eq. (5), [6]:

$$V_{OC,T} = V_{OC,STC}\left[1 + \frac{\Delta V_{OC}}{100}(T - 25)\right]. \quad (5)$$

Temperature coefficient for open circuit voltage changing for PV module YL235P-29b is $\Delta V_{OC} = -0{,}37\,\%/^0\text{C}$. According to this data and Eq. (5) for cells temperature T=−10 ^{0}C, $\Delta V_{OC,-10} = 41{,}8$ V.

For 15 serial connected PV modules input DC voltage to the inverter will be $U_{PV,15} = 15 \times 41{,}8 = 627{,}0$ V whereas for 16 PV modules will be $U_{PV,16} = 16 \times 41{,}8 = 668{,}8$ V. It is obvious that in both cases the input DC voltage to the inverter don't exceed 700 V.

According to the technical data for the inverter SMA SMC 11000TL maximal power on the DC input (from PV generator side) is 11400 W. In real working conditions PV module maximum (peak) power cannot be greater than power on STC. For the proposed PV module YL235P-29b this power is 235 Wp. In case for 15 PV modules, the peak power of a string is $15 \times 235 = 3525$ Wp whereas in case for 16 PV modules $16 \times 235 = 3760$ Wp. Technically it is possible to connect 5 strings to the proposed inverter. However, taking into account before explained voltage and maximal DC input power limits for the chosen type of PV modules, the optimal number of strings that can be connected to the inverter is 3. Therefore, the PV generator should be constructed with 3 strings connected in parallel with same number of PV modules per string.

In case for 15 PV modules per string the peak power to the inverter DC input will be $3 \times 3525 = 10575$ Wp whereas in case for 16 PV modules per string $3 \times 3760 = 11280$ Wp. The main purpose in PVP designing is to obtain the maximum active power from the inverter as it is possible. According the above conducted considerations the optimal number of PV modules per string is 16 (Fig. 4 a)) and optimal number of parallel strings connected on inverter DC input is 3 (Fig. 4 b)).

Finally, it is necessary to check if the current of calculated number and configuration of modules and strings doesn't exceed limited maximal current of the inverter. According to the technical data in Table II, for the proposed inverter value of this current is $I_{PV,\max} = 34$ A. Maximal current which can flow through a string is short current of PV modules.

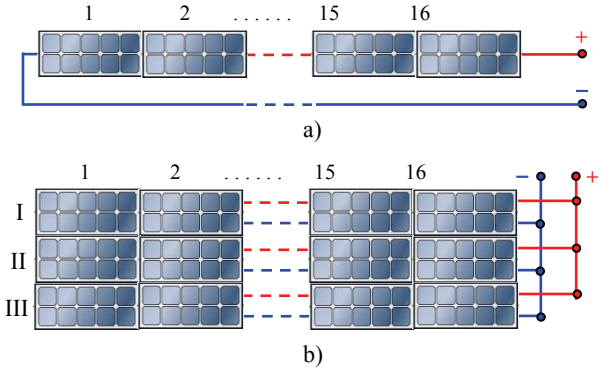

Fig. 4. a) String with 16 PV modules b) PV generator with 3 strings.

During the calculations it can be taken into account that the value of this current rises when the cells temperature rise. For the proposed PV module the short current is $I_{SC,STC} = 8{,}54$ A on STC and temperature coefficient is $\Delta I_{SC} = 0{,}06\,\%/^0\text{C}$. Short current value for cells temperature T=70 ^{0}C can be calculated according Eq. (6), [6]:

$$I_{SC,T} = I_{SC,STC}\left[1+\frac{\Delta I_{SC}}{100}(T-25)\right]. \qquad (6)$$

With the above adequate quantities and applying Eq. (6) the PV module short current (which is the same as a string short current) $I_{SC,70} = 8{,}77$ A is calculated.

Because the PV generator is consist of 3 parallel connected strings maximum current in the inverter DC input can be short current of the PV generator or $3\times 8{,}77 = 26{,}31$ A. Therefore, the inverter maximum DC input current of 34 A (Table II) will not be exceed. Taking into account all considerations it can be conclude that 3 parallel connected strings with 16 PV modules per string is optimal combination from the aspect of maximum gained active power for certain solar radiation intensity. This combination of PV modules and strings totally satisfy all limitations and recommendations for accepted PV modules YL235P-29 and inverter SMA SMC 11000TL.

IV. Conclusion

During the designing and construction of PVP it is necessary to gain maximum power from the chosen equipment for certain solar radiation intensity. Beside selection the quality equipment, it is required to match optimal PV generator parameters with the inverter parameters. In this paper is presented a way for determination of optimal photovoltaic modules number in a string and optimal strings number connected into inverter for active power maximization. All limiting factors of the inverter as: MPPT device working voltages, maximal permitted voltage and current are taken into account. On a real case of chosen types of PV module and inverter are performed calculations. Step by step is explained way of calculations applying technical data of PV module and inverter. The obtained results are analyzed and commented.

References

[1] V. Mijalović, "*Distribuirani izvori energije – principi rada i eksploatacioni aspekti*", Akademska misao, Beograd, 2011.

[2] Team of ICEIM-MANU, *Base study for use of renewable energy sources in R. Macedonia until 2020*, Government of R. Macedonia, Skopje, 2010.

[3] Team of ICEIM-MANU, *Strategy for energy sector development in R. Macedonia until 2030*, Government of R. Macedonia, 2010.

[4] Yjngli Solar YL 235 P-29b / 1650x990 Series, Technical Data, Yingli Green Energy Holding Co. LTD.

[5] Sunny Mini Central SMC 11000TL, Technical Data, SMA Solar Technology AG, Germany.

[6] DGS Berlin, "*Planning and Installing Photovoltaic Systems. A guide for installers, architects and engineers*", Second Edition, Earthscan, ISBN 978-1-84407-442-6, London, 2008.

Transient Stability of Asynchronous Generator on Distribution Network

Metodija Atanasovski[1], Mitko Kostov, Nikola Acevski, Blagoj Arapinoski, Elena Kotevska

Abstract – **Dispersed generation (DG) brings together wide range of technologies for electricity production. Most frequently used electric machines for electricity production at each technology that belongs to DG group are: synchronous generators, asynchronous generators (AG) and power converters. This paper deals with transient stability of AG. Typical model of distribution network (DN) is developed with AG connected to it. The modelling and simulation are performd with NEPLAN and MATLAB/SIMULINK/Simpowersystems toolbox software packages. AG with squirrel cage is used. Several short circuits are simulated in order to investigate dynamic behaviour of AG. Following parameters are analyzed: rotor speed, active and reactive power, and currents of AG. Critical clearing time is calculated for keeping stable operation of AG. Several useful and practical conclusions are obtained.**

Keywords – **Asynchronous generator, Transient stability, Distribution network.**

I. INTRODUCTION

Last decade of past century bring remarkably revival of interest for connection generation units to DN. This phenomena in power systems is called dispersed generation. The term dispersed is introduced to make a difference with conventional centralized generation usually connected on transmission network. The story of DG is not a new one. Construction of small generating units is well known long ago from the beginning of power systems industry [1].

The installed capacity of DG is a key factor for obtaining voltage level for its connection to DN. Voltage levels for DG connection are the typical distribution voltage levels which vary from 400 V up to 110 kV [2].

DG category definition is not based on primary source used for electricity generation, but it is based on its technical performances from power system point of view. DG brings together wide range of technologies for electricity production. Most frequently used electric machines for electricity production at each technology that belongs to DG group are: synchronous generators, asynchronous generators (AG) and power converters (dc/ac or vice versa). AGs are mostly used at wind farms, small and medium size hydro power plants [2].

The problem of transient stability on DN becomes very interesting with increased presence of DG. Reasons about this can be summarized as: investigation of generators behaviour on DN and their impact on it, calculation of critical clearing time for remaining generator stable operation and impact of generators transient stability on networks protection.

This paper deals with transient stability of AG. Typical model of distribution network is developed with AG connected to it. The paper is consisted of four sections. Concept and model of AG for transient stability analysis is explained in section II. Also critical clearing time for stable operation is defined. The modelling and simulation are performed with NEPLAN and MATLAB /SIMULINK/ Simpowersystems toolbox software packages. AG with squirrel cage is used. Obtained results from performed simulations are depicted in section III. Three phase and two phase short circuits are simulated in order to investigate dynamic behaviour of this type of generators. Following parameters are analyzed: rotor speed, active and reactive power, and currents of AG. Critical clearing time is calculated for keeping stable operation of AG. Several useful and practical conclusions are obtained and elaborated in section IV.

II. DISTRIBUTION NETWORK MODEL WITH ASYNCHRONOUS GENERATOR

DG transient stability studies are similar to large scale power system transient stability studies, except that DG capacity is normally very small relative to the bulk system and has no significant influence on its frequency or stability. The research is performed for DG that uses AG as electric machine. Practically the purpose is to investigate the ability of AG unit to remain synchronized and determining its critical clearing time, when feeder disturbance occurred on the DN.

The concept of critical clearing time in the case of synchronous generator is well known. Unlike synchronous generators, AGs do not have field windings to develop the required electro-magnetic field in the machine's air-gap. Therefore, AGs can not work with out external power supply. The electro-magnetic torque (T_e) developed inside an induction machine at any given speed is proportional to the square of the terminal voltage as follows [3]:

$$T_e = K \cdot s \cdot U^2 \tag{1}$$

Where K is constant value depends on the parameters of the machine, s is the machine slip.

Electro-magnetic torque is, therefore, bound to reduce following a fault condition, proportionally to square of voltage. On the other hand, the dynamic behavior of the rotor is governed by the swing equation given below:

[1]Metodija Atanasovski, Mitko Kostov, Nikolace Acevski, Blagoja Arapinovski and Elena Kotevska are with the Faculty of Technical Sciences-Bitola, University St. Kliment Ohridski, Republic of Macedonia, E-mail: metodija.atanasovski@tfb.uklo.edu.mk.

$$J\frac{dw}{dt} = T_m - T_e \quad (2)$$

Where: J is moment of inertia of the rotating mass, T_m is the mechanical torque applied on rotor of the associated wind or hydro turbine, w is rotor speed.

It can be concluded from (2) that assuming the mechanical torque is kept constant, then any reduction in the electro-magnetic torque, for instance due to fault condition, causes the rotor to accelerate. This in turn leads to an increase in the kinetic energy of the rotating mass. When the fault is cleared and consequently system voltage recovers, the magnetic field inside the air-gap of the machine starts to build up. This causes high inrush current to be drowned by the machine from the network which in turn causes a voltage drop across the interfacing link between the AG and the substation leading to a reduction in the voltage at the generator terminals. The resulting electro-magnetic torque acts on the rotor in a direction opposite to that of mechanical torque applied by turbine. If the energy stored in the newly established rotating magnetic field becomes higher than that stored in the rotating mass, rotor speed is forced to slow down and the generator eventually retains its normal operating condition following few oscillations, otherwise, its speed continues to increase until it is tripped by appropriate protection devices. When this is happening generator terminals usually experience sustained voltage dip. This investigation has shown that there is a maximum time for the fault to be cleared, otherwise AG losses its stability. Such time will thereafter be referred to as the critical clearing time for AG [4].

III. SIMULATION AND RESULTS

Study case analyzed in this paper is shown on Fig. 1. It consists of DN with AG of 1 MVA rated power. The modelling and simulation are performed with NEPLAN [5] and MATLAB /SIMULINK/ Simpowersystems toolbox [6] software packages. AG with squirrel cage is used which is represented with fourth and sixth order model for transient stability. Mechanical moment (power) of prime mover (turbine) is considered constant to achieve greater generics of results. Part of the reactive power consumed by AG is supplied locally with model of capacitor.

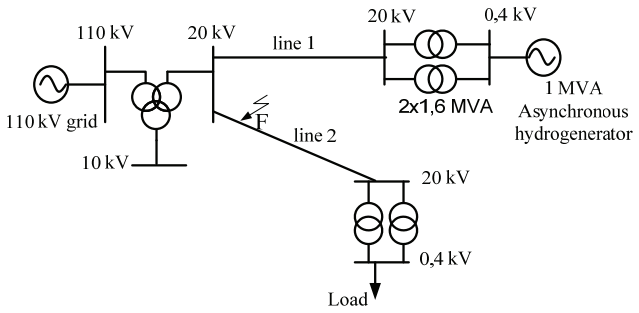

Fig.1. Schematic diagram of the case study DN with AG

Generator is integrated into the DN at 20 kV voltage level through 2x1.6 MVA 0.4/20 kV/kV step-up transformers and 20 kV distribution line 1. 110 kV network is represented by infinite model with voltage source behind its Thevenin's equivalent impedance. The fault level of the 110 grid is assumed 5000 MVA. HV/MV substation is represented by three windings transformer 110/20/10 kV/kV/kV and 31,5/31,5/10,5 MVA/MVA/MVA. The load is connected to the substation through distribution line 2 and 20/0,4 kV/kV transformers. Load characteristic is represented with constant impedance model. Both lines 1 and 2 are simulated with π-equivalent circuit with impedance of $(0.413 + j0.36)\Omega/km$. All transformers are modeled in a same way as in short circuit calculations.

Simulations are performed for three and two phase short circuits at location F (see Fig. 1), located on 20 % of line 2 length measured from substation HV/MV/MV. Results for three phase fault duration of 70 ms are shown on Fig. 2. The corresponding AG rotor speed is shown on Fig. 2(a), active power of AG on 2(b) and reactive power on 2(c).

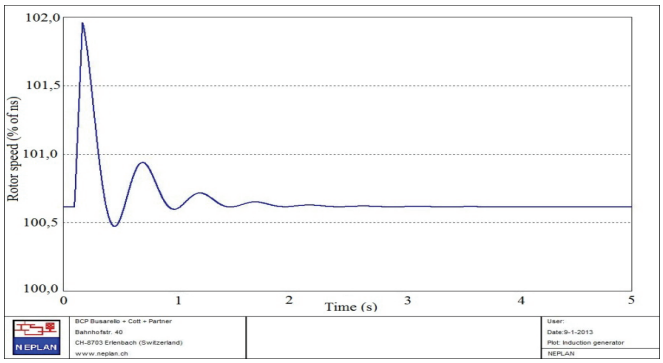

a)

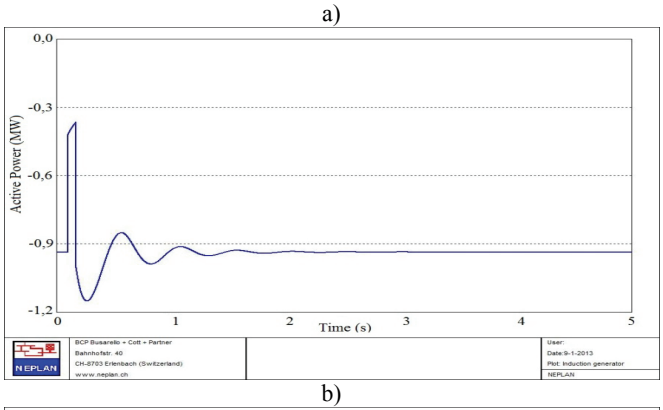

b)

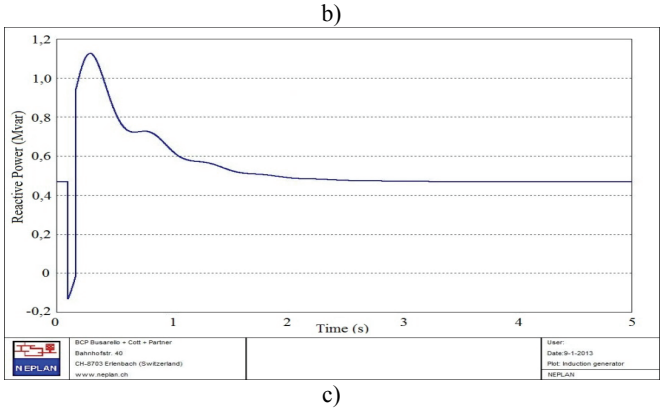

c)

Fig. 2. Simulation of three phase fault at location F with duration of 70 ms; a) Rotor speed of AG in %, b) Active power of AG, c) Reactive power of AG.

Fig. 2a) shows that rotor speed retains stable position through few oscillations after fault clearance. Analyzing Fig. 2b) it is obvious that AG active power has dropped to 40 % of its nominal value during fault duration, but after short circuit is cleared active power retained its normal operational value. Fig. 2c) depicts reactive power variation of AG.

The different behavior of each generator can be explained by analyzing the response of the reactive power exchanged between the generator and the network for each situation. In the case of the induction generator, the reactive power exchanged takes into account the reactive power supplied by the capacitors. When fault occurs (Fig. 2c)) AG for a fault duration injects reactive power into the network due to self-excitation phenomenon, but, soon after fault clearance, AG consumes a large amount of reactive power, which can lead the system to a voltage collapse if it is not disconnected quickly with fast response of protection.

Due to this response of reactive power of AG, its small critical clearance time can be explained. Namely, after several repeated simulations by increasing fault duration time, critical clearance time of AG is calculated to be 100 ms. Fig. 3 shows rotor speed behaviour due to fault duration of 130 ms. It is obvious that AG is unstable and its rotor speed continuously increase until protective devices disconnect AG from the network.

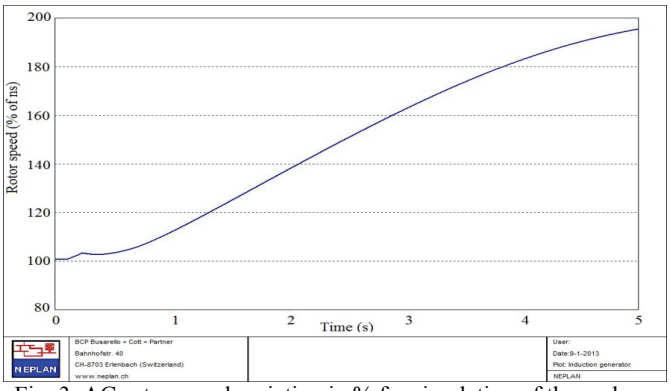

Fig. 3. AG rotor speed variation in % for simulation of three phase fault at location F with duration of 130 ms

The same DN from Fig. 1 is also modeled using program for analysis electromagnetic transients. MATLAB SIMULINK/Simpowersystems toolbox is used for investigating the response of AG phase currents to symmetrical and asymmetrical short circuits in DN. Three phase model of network elements is developed and simulations are performed in continuous time domain. Previous simulations in NEPLAN are done in phasor domain which is usually used for transient stability analysis.

For purposes of these simulations at location F three and two phase short circuits are applied. Fig. 4 and Fig. 5 show AG stator phase currents behavior for three and two phase short circuit appropriately. Analyzing stator phase currents of AG for three phase short circuit (Fig. 4) at location F occurred at t=50 ms, it can be seen that initially current magnitude is high but, it decrease quickly because this machine has no capacity to provide sustained short-circuit currents during three-phase faults. Voltages (phase or line to line) on AG

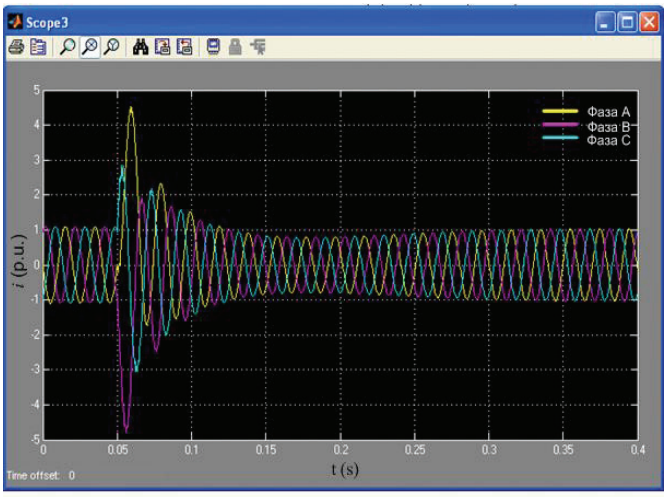

Fig. 4. Stator phase currents of AG for three phase short circuit at location F

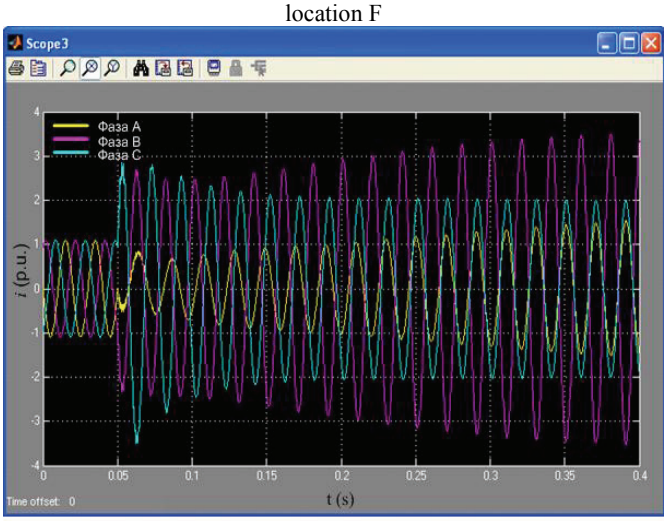

Fig. 5. Stator phase currents of AG for two phase short circuit at location F

terminals drop on 30 % of their nominal value. If short circuit occurs on AG terminals voltages drop to zero and the capacitor bank becomes unloaded. Consequently, there is no external excitation source for the generator, and it becomes unable to produce voltage. Theoretically, this fact could become the detection of faults by protection systems based on over-current relays more difficult. However, in this case, voltage-based relays could be used.

Analyzing AG stator phase currents for two phase short circuit (Fig. 5) at location F occurred at t=50 ms, it can be concluded that AG current response demonstrates capacity for sustainable supply of short circuit current. All three phases remain excited by the network. Currents at faulted phases B and C present sustained response, although current at healthy phase A also shows sustainable increase of its amplitude.

IV. Conclusion

Dynamic behaviour of AG connected on DN is investigated in the paper. It can be concluded that AG has very low critical clearing time to remain its stability during fault in the

network. Reasons for this phenomenon are in reactive power response during fault occurrence and after its clearance.

Performed simulations have clearly shown that current response of AG is with high amplitudes of currents at all phases in the moment of three phase short circuit (symmetrical short circuit) occurrence. However, currents rapidly decrease because AG has no capacity to provide sustained supply of short-circuit currents during three-phase faults. This fact imposes conclusion that in networks which have reached circuit breakers breaking current limit, AG can be used in DG installations. For asymmetrical short circuits, current response of AG has capacity to provide sustained supply of short-circuit currents.

Comparison of AG dynamic behavior with synchronous generator is very important for determination of there advantages and disadvantages from DN stand point of view. This conclusion suggests further investigation about this matter. Synchronous generator can be applied on the same network model for obtaining its dynamic performance and critical clearing time for same fault conditions in DN.

REFERENCES

[1] Atanasovski M., Taleski R., "Power Summation Method for Loss Allocation in Radial Distribution Networks With DG," *IEEE Trans. on Power Systems*, Vol. 26, No. 4, pp. 2491−2499, November 2011.

[2] Nick Jenkins, Ron Allan, Peter Crossley, Daniel Kirschen and Goran Strbac: *EMBEDDED GENERATION*, Published by The IEE, London, United Kingdom, 2000.

[3] Salman K. S., Ibrahim M. Rida. "Investigating the Impact of Embedded Generation on Relay Settings of Utilities Electrical Feeders." *IEEE Tran.s on Power Delivery*. Vol. 16, No. 2, pp. 246-251, April 2001.

[4] Walmir Freitas, J. C. M. Vieira, A. Morelato, L. C. P. da Silva, V. F. da Costa, F. A. B. Lemos. "Comparative Analysis Between Synchronous and Induction Machines for Distributed Generation Applications". *IEEE Tran.s on Power Systems,* Vol. 21, No.1, pp. 301−311. February 2006.

[5] NEPLAN User's Guide V5, BCP BCP, www.neplan.ch.

[6] User's Guide MATLAB/SIMULINK/SimPowersystems Toolbox, version 3, The MATHWORKS, 2003.

Economic Energy Scheduling of an Islanded Microgrid

Galia Marinova[1] and Vassil Guliashki[2]

Abstract – **This paper considers the calculation of an effective energy schedule in an islanded microgrid. GridLab-D open source simulation tool is used to for simulation of microgrid elements. Matlab environment is used to run an optimization solver. The product GridMat is used as an interface tool between Matlab and GridLab-D. An economic scheduling optimization problem on the considered microgrid is formulated and solved.**

Keywords – **Microgrids, GridLab-D, GridMat, Matlab, Energy scheduling optimization.**

I. INTRODUCTION

A microgrid represents a low-voltage distribution system consisting of distributed energy resources (DERs) or renewable energy resources (RES) and controllable loads, which can be used/controlled in either islanded or grid-connected mode. The microgrid should be robust in controlling supply, demand, voltage, and frequency. The DERs/RES production plan can be evaluated by using meteorological forecasts, which have an intrinsic uncertainty. In such a setup, energy storage can help in meeting the hourly production plan [2].

In this paper the microgrid economic scheduling is studied, i.e. the problem to optimize the energy storage/battery schedule, as well the schedule of the diesel generator used, covering the time-varying energy demand and operational constraints while minimizing the costs of internal generated energy. The experimental microgrid includes a photovoltaic system, a wind turbine, a diesel generator and three houses. The microgrid's point of common coupling (PCC) is disconnected from the main grid and the microgrid operates in an island mode. Formulating an optimization task the amount of power demand and supply for the next 24 hour period may be assumed to be known without any change. This is an unrealistic setup, especially in real world applications.. Also the solar radiation forecasts could be inexact and could vary essentially. For this reason the energy, generated by the diesel generator should include a reserve rate (see [5, 6]) and the forecasted data for the renewable energy resources (wind turbine and photovoltaic system), as well as for the loads (houses) should be taken adding a safe margin for each microgrid elemet.

The open source GridLab-D (see [3]) is used to simulate all the elements of the microgrid. The software product GridMat (see [1]) is used as an interface tool between Matlab (see [4]) and GridLab-D. Climate data, available on the official website of GridLab-D, are used for the simulations. The optimization problem is formulated and solved in an efficient way by using the Matlab optimization toolboxes/solvers.

[1]Galia Marinova is with the Faculty of Telecommunications at Technical University of Sofia, 8 Kl. Ohridski Blvd, Sofia 1000, Bulgaria, E-mail: gim@tu-sofia.bg.

[2]Vassil Guliashki is with the Institute of Information and Communication Technologies – BAS, "Acad. G. Bonchev" Str. Bl. 2, 1113 Sofia, Bulgaria, E-mail: vggul@yahoo.com.

II. THE EXPERIMENTAL MICROGRID

The microgrid studied in this work, is composed by several units which produce, exchange and consume energy. Essentially, the microgrid operates with a three-phase medium voltage alternating current (AC) transmission system, which can be connected or not to the main grid (Network) through a transformer system, in order to buy the energy necessary to cover the demand, or sell the surplus energy produced by the RES. When the microgrid is used in an Island mode (disconnected from the Network), a diesel generator is considered in order to supply, together with the RES, the energy necessary to cover the loads. Two type of RES are considered connected in the Microgrid: 1) a photovoltaic system composed by an inverter and a group of solar panels, and 2) a wind turbine. A group of batteries (energy storage system) is also interconnected to the microgrid through a DC/AC bi-directional inverter. This is exactly the part that makes the microgrid under study a *smart* microgrid, since the schedule of batteries is based on the behavior of the loads and the energy production by the RES. The system configuration of the proposed microgrid is presented on Fig. 1:

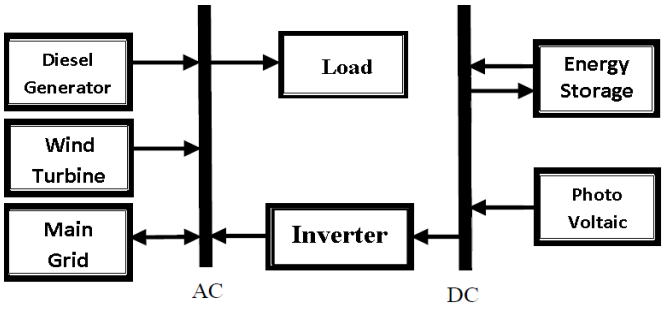

Fig. 1. Microgrid system configuration

The microgrid with all its components is shown on Fig 2.

III. ECONOMIC SCHEDULING OPTIMIZATION MODEL

It this study the behavior of the RES and houses has been simulated from historical climate data of a particular geographical position: Seattle (USA); The data for solar radiation and wind speed, as well for the houses energy consumption are real data for a given winter day. They are taken as a forecasted data.

In [5] are given energy safety margins necessary to cover the uncertainty of the forecasted data. Taking into account these margin values, in the created optimization model are assumed the following values: Wind turbine: (–30%) ;

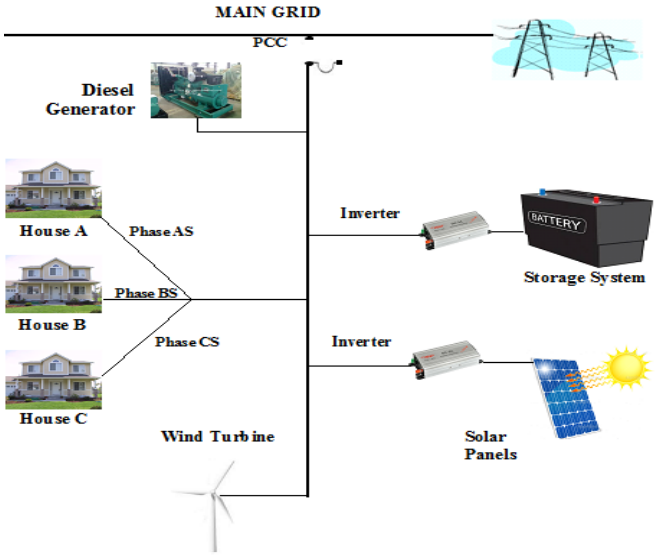

Fig. 2. The experimental microgrid

Photovoltaic: (–37%); Houses: (+25%); Diesel generator: (+20%). Having available correct forecasted data for the RES production and houses consumption one day before for the next day, it is possible to optimize the microgrid behavior for a whole year, solving one day ahead the correspondent scheduling optimization problem for the next day.

The time interval being analysed (one day and one night) is divided by 24 time steps, each with 1 hour length. The balance power P_B of the studied microgrid should satisfy the following equations (see [6]):

$$P_{RES} + P_B = P_L \quad (1)$$

$$P_B = P_{Bat\_d} + P_{DG}\,, \quad (2)$$

where P_{RES} is the output power of renewable energy sources, P_B is the balance power, P_{Bat_d} is the power from discharging the battery system, P_{DG} is the output of the diesel generator, and P_L is the microgrid load, equal to houses consumption energy plus battery system charging energy. The parameters and the decision variables used are presented in Table 1.

TABLE 1. PARAMETERS

Parameter	Description
CS	Capital cost for interval of one hour
OM	Operation maintenance for one hour
RC	Replacement cost (of the battery)
FC	Fuel cost for interval of one hour
EC	Emission cost for interval of one hour
CRF	Capital recovery factor for one hour
SFF	Sinking fund factor for one hour

Taking into account that the photovoltaic area, the wind turbine capacity, as well as the house energy consumption cannot be subject to optimization since their schedules are independent, the objective function includes the balance power:

$$\min \boldsymbol{F} = \sum_{t=1}^{24}(C_t.P_{Bt}) = \sum_{t=1}^{24} CC_{DG}(t) + OM_{DG}(t) + FC_{DG}(t) + EC_{DG}(t) + \sum_{t=1}^{24} OM_{Bat}(t) + RC_{Bat}(t) + CC_{Inv}(t) \quad (3)$$

where P_{Bt} is the balance power for hour t and C_t is the cost of this power. In C_t are included the deprecations costs of each microgrid energy generation element (unit), of operational costs of individual units, of the fuel cost (for the fuel consumed by the diesel generator), and of emission cost. Calculating $\boldsymbol{F}$ only the hours, when the diesel generator operates and when the battery system is charging/discharging are taken into account. In [9, 10] are given formulas for calculating the correspondent annual values. Hence the one hour capital cost of microgrid units, which do not need a replacement during the project life time, such like diesel generator and inverter, is calculated as follows:

$$CC_{DG} = \frac{Ccap_{DG}.\mathrm{CRF}(i, \mathrm{y})}{5375}, \quad (4)$$

Assuming, that the diesel generator is used average 15 hours in a 24 h period, the denominator is: 5375 = 15 × 365;

$$\mathrm{CRF}(i, \mathrm{y}) = \frac{i.(1+i)^{\mathrm{y}}}{(1+i)^{\mathrm{y}} - 1} \quad (5)$$

Here $Ccap_{DG}$. is the capital cost (US$), y is the project life time, and i is the annual interest rate [11]:

$$i = \frac{i' - f}{1+f} \quad (6)$$

where: i' is the loan interest (%), and f is the annual inflation rate (%).

The one hour operation maintenance cost is:

$$OM = \frac{Ccap_{DG}.(1-\lambda)}{5375.\mathrm{y}} \quad (7)$$

for the diesel generator, and

$$OM = \frac{Ccap_{Bat}.(1-\lambda)}{6570.\mathrm{y}} \quad (8)$$

for the battery, where: λ is the reliability of correspondent unit.

Assuming, that the battery bank is used average 18 hours in a 24 h period (i.e. 365 × 18 = 6570 hours annually), the one hour battery bank replacement cost is:

$$RC = \frac{Crep_{Bat}.\mathrm{SFF}(i, y_{rep})}{6570} \quad (9)$$

where: *Crep* is the replacement cost of battery bank, and SFF is the sinking fund factor, which is calculated as follows [11]:

$$\mathrm{SFF} = \frac{i}{(1+i)^{\mathrm{y}} - 1} \quad (10)$$

The one hour fuel cost of diesel generator for hour t is:

$$FC = Cf.G(t)$$

where: Cf is the fuel cost per liter, and $G(t)$ is the hourly consumption of diesel generator [7, 8, 9, 10] as follows:

$$G(t) = (0{,}246P_{DG}(t) + 0{,}08415.P_R) \quad (11)$$

where: $P_{DG}(t)$ is the diesel power at time t, and P_R is the rated power of the diesel generator.

The hourly emission cost (CO_2 emission) is:

$$EC(\mathrm{t}) = \frac{E_f.E_{cf}.P_{DG}(t)}{1000} = 0{,}0187.P_{DG}(t) \quad (12)$$

where: E_f is the emission function (kg/kWh), and E_{cf} is the emission cost factor ($/ton)

The necessary economic data are given in Table 2:

Table 2. THE ECONOMIC DATA

Interest rate *i*' (%)	3
Inflation rate (%)	1,6
Inverter life time (years)	20
Battery life time (years)	10
Reliability of inverter (%)	0,98
Reliability of battery (%)	0,98
Reliability of diesel (%)	0,9
Cost of diesel generator (US$/KW)	500
Cost of battery bank (US$/KWh)	200
Cost of inverter (US$/KW)	1000
Fuel cost (*Cf*) (US$/l)	0,75
Emission function (kg/kWh)	0,34
Emission cost factor (US$/ton)	55

Other parameters to be defined are the Pbt_max , fixed to 10 kW for charging and discharging, and E_{bt_max}, fixed to 100 kWh. The data in Table 3 are taken from [9], only the fuel cost value is taken from [10]. Since P_R = 38, hence $Ccap_{DG}$ = 19000 $. In [6] is stated, that the high speed (3600 r/min), air-cooled diesel can be used for about 20 000 h. Hence y in formulas (5), (7) and (8) is: y = 3,721. The annual interest rate i = 0,53846154. Hence CRF(i, y) = 0,6742. CC_{DG} = 2,38 $/h. OM_{DG} = 0,095 $/h. OM_{Bat} = 0,0061 $/h. $Crep_{Bat}$ = 20000 $. SFF = 0,1357. RC = 0,413 $/h. $Ccap_{Inv}$ = 10000. The inverter one hour capital cost is: CC_{Inv} = 1 $/h.

Hence the objective function (3) is presented in the form:

$$\min \boldsymbol{F} =$$

$$= \sum_{t=1}^{24} 2{,}38_{DG}(t) + 0{,}095_{DG}(t) + 0{,}1845.P_{DG}(t) + 2{,}398_{DG}(t) + \quad (13)$$

$$+ 0{,}0187.P_{DG}(t) + \sum_{t=1}^{24} 0{,}274_{Bat}(t) + 0{,}413_{Bat}(t) + 1_{Inv}(t)$$

The constraints concerning the diesel generator are:

$$0{,}3.P_R \le P_{DG}(t) \le P_R \quad (14)$$

Taking into account the modified values from [5], the following constraint is obtained:

$$P_{DG}(t) = \begin{cases} 1{,}2.(1{,}25.P_L - 0{,}63.P_{PV} - 0{,}7.P_{WT} - P_{Bat\_d}) \\ \quad if \;\; 0{,}63.P_{PV} + 0{,}7.P_{WT} + P_{Bat\_d} < 1{,}25.P_L \\ 0. \qquad\qquad\qquad\qquad otherwise \end{cases} \quad (15)$$

The constraints concerning the battery system are:

$$-P_{bt\_max} \le P_{\mathrm{Bat}}(t) \le +P_{bt\_max} \quad (16)$$

$$SOC_{min} \le SOC(i) \le SOC_{max} \quad (17)$$

$$\sum_{t=1}^{24} P_{Bat}(t) = 0; \quad t = 1,...,24; \quad (18)$$

where: $P_L(t)$ is the power absorbed by the houses during the hour "t" [kW]; $P_{PV}(t)$ is the power delivered by photovoltaic panels during the hour "t" [kW]; $P_{WT}(i)$ is the power delivered by wind turbine during the hour "t" [kW]; $P_{Bat\_d}(t)$ is the power delivered by the battery block (discharging) during the hour "t" [kW]. *Pbt_max* is the maximum power that the battery system can deliver/absorb [kW]; $SOC(t)$ is the State Of Charge of the battery during the hour "t" [%] SOC_{min} = lower limit for the State Of Charge of the battery [%] SOC_{max} = upper limit for the State Of Charge of the battery [%].

Finally taking into account the energy balance of the microgrid (see equations (1)-(2)), the last constraint obtained is:

$$P_{Bat}(t) + P_{DG}(t) \ge P_H(t) - P_{PV}(t) - P_{WT}(t)\,,\; t = 1,...,24; \quad (19)$$

where $P_H(t)$ is the house consumption energy. The energy $P_{Bat}(t)$ is considered positive when the battery is discharging and negative when is charging. Therefore, the equation (16) represents the power limit, which can be delivered or absorbed by the inverter tie to the battery system; the system cannot supply or absorb a power more than the *Pbt_max*.

The SOC of the battery represents the amount of energy stored in the battery system. Therefore, the equation (17) means that, for each time step, the SOC must be included between a minimum and a maximum value depending by the system used to storage the energy and agree with physical limit of maximum SOC of 100%. In this case, the minimum and maximum level of SOC are fixed to 20% and 100% respectively.

The SOC is depending on the value of $P_{Bat}(t)$ for each time step; the relation between these variables is shown below:

$$SOC(t) = SOC(t-1) - \frac{P_{Bat}(t)}{E_{bt\_\max}}.\Delta t \quad (20)$$

where: Δt is the time step [h], $SOC(0)$ = Initial charge of the battery (it is an input value of the problem). In this optimization problem, the initial value of the SOC is fixed to 50%. It means that, at the begin of the optimization, the battery system is charged to the half of its full charge.

The constraint, shown in equation (18), is used in order to get, at the end of the 24h period, the same value of SOC like at the begin of the period.

IV. TEST RESULTS OBTAINED BY MEANS OF THE SIMULATION AND THE OPTIMIZATION TOOLS

The simulations with GridLab-D give the results about the consumption of the houses, the production of the solar panels and wind turbine. The results obtained from the simulations, for a winter day, are shown on Fig. 3.

The problem (13)-(19) has 48 variables: $P_{DG}(t)$ and $P_{Bat}(t)$, t=1,…,24; To solve this optimization problem, the Matlab solver *fmincon* has been used. In the *"Help"* menu in Matlab, in the "Optimization Toolbox" the description and explanation how to run this solver is given.

The first 24 variables on Fig. 4 represent the battery schedule, and the next 24 variables correspond to the diesel generator schedule.

The calculated optimal schedule for the battery system is:

[-10. -10. -100 1.3786 10. -10. -1.1083 10. 10. -10. -10.
-10. 9.7297 -10. -10. 10. 10. 10. 10. -10. 10. 10. 10. -10.]

The calculated optimal schedule for the diesel generator is:

[11.4 11.4 11.4 11.4 0. 11.4 22.0169 32.5701 22.3065
17.9062 14.4096 11.5544 0. 11.4 11.4 0. 18.4714 25.1381
29.1214 28.5803 26.6152 24.9310 20.7732 13.0999].

The optimization result shows, that the total cost for 24h period for a winter day, based on the objective function (13) IS: $\boldsymbol{F}$ = 205,037. Without optimization for an initial battery schedule: $P_{Bat}(0)$ = [0 0 0 -0.8 -0.8 -0.8 -0.8 -0.8 -1 0 1 1 1 1 1

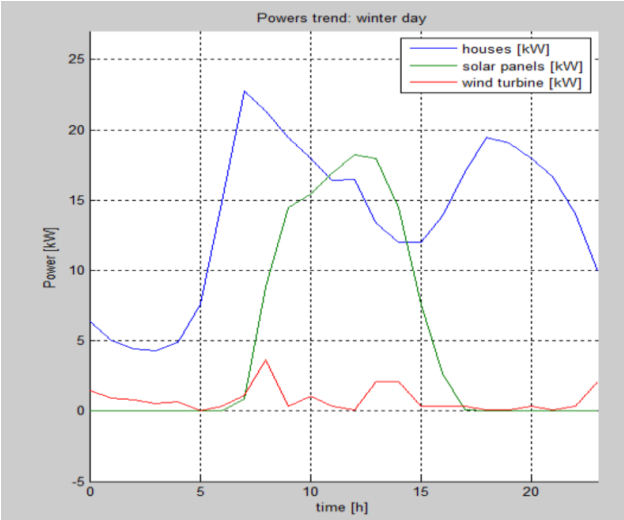

Fig 3. Houses consumption, solar panels and wind turbine energy generation for a winter day

The results of running "*fmincon*" for a winter day using the "*optimtool*" command in Matlab are shown on Fig. 4.

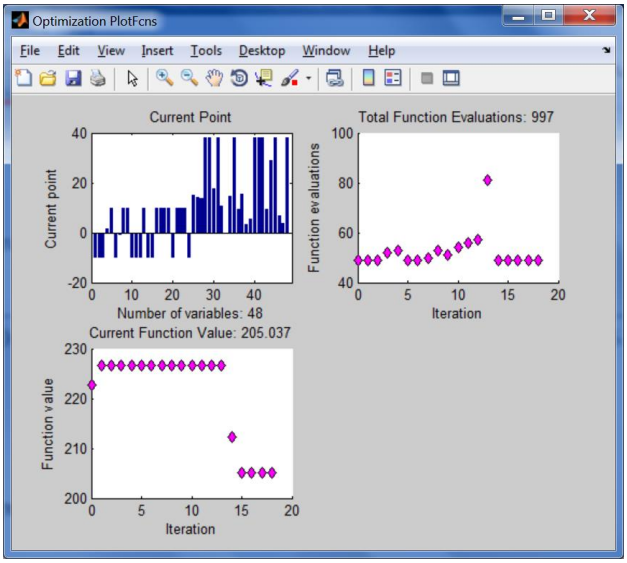

Fig. 4. Optimization result from "*fmincon*" solver

-0.8 -0.8 -0.8 -0.8 -0.8 -1 1 2 2] the objective function value is ***F*** = 226,717. Hence the optimization of battery schedule and diesel generator schedule simultaneously leads to about 10,574% reduction of necessary costs.

V. Conclusion

An optimization of a battery and diesel generator schedule in a microgrid is presented in this paper. Using the solution for the schedules two goals are achieved: 1) It is guaranteed that the load demand is covered by an enough high reserve. 2) The optimization leads to 10,574% reduction of the necessary costs. At the same time the costs for the end user are essentially reduced. Minimizing the objective function, the fuel consumption by the diesel generator is minimized, as well and the harmful impact on the environment is also reduced.

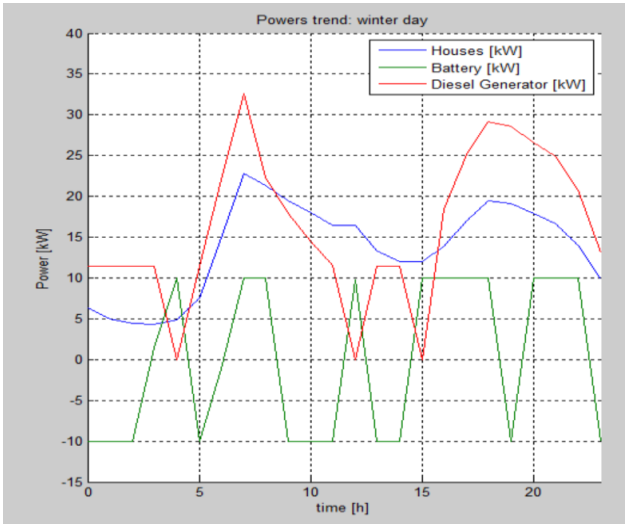

Fig. 5. Graphics of Houses consumption, optimized Battery schedule and optimized Diesel generator schedule

References

[1] Al Faruque M. A., F. Ahourai : "GridMat: Matlab Toolbox for GridLAB-D to Analyse Grid Impact and Validate Residential Microgrid Level Energy Management Algorithms", IEEE PES Conference on Innovative Smart Grid Technologies (ISGT'14), Washington DC, USA, February 2014. http://aicps.eng.uci.edu/papers/GridMat-ISGT-2014.pdf

[2] Marinelli M., "Testing of a Predictive Control Strategy for Balancing," *IEEE TRANSACTIONS ON SUSTAINABLE ENERGY,* 2014.

[3] Chassin, D. P., "GridLAB-D: An agent-based simulation framework for smart grids," 13 May 2014.

[4] Matlab, [Online]. http://www.mathworks.com/products/matlab/

[5] Chang G. W, H. J. Lu, H. J. Su, "Short-term Distributed Energy Resource Scheduling for a DC Microgrid," *Energy and Power Engineering*, 2013, vol. 5, pp. 15-21.

[6] Xiao J., L. Bai, F. Li, H. Liang, and C. Wang, "Sizing of Energy Storage and Diesel Generators in an Isolated Microgrid Using Discrete Fourier Transform (DFT)", *IEEE Transactions on Sustainable Energy*, Vol. 5, No. 3, July 2014

[7] Dufo-Lopez R. and J. L. Bernal-Agustin, "Multi-objective design of PV-Wind-Diesel-Hydrogen-Battery systems", accepted for publication in *Renewable Energy* (http://www.sciencedirect.com/science/journal/09601481)

[8] Skarstein O, Ulhen K., "Design Considerations with Respect to Long-Term Diesel Saving in Wind/Diesel Plants", *Wind Engineering* 1989; 13(2):72–87.

[9] Luu**,** N. A., "Control and management strategies for a microgrid", Ph.D. Thesis, Université de Grenoble, France, 18.12.2014, https://tel.archives-ouvertes.fr/tel-01144941/document

[10] Seryoatmojo H., A. A. Elbaset, Syafaruddin and T. Hiyama, Genetic Algorithm based optimal sizing of PV-Diesel-Battery System, Considering CO2 Emission and Reliability, *International Journal of Innovative Computing, Information and Control*, Vol. 6, No. 10, October 2010, 1-09-0844, ISSN: 1349-1198.

[11] Diaf S., M. Belhamelb, M. Haddadic, A. Louchea, Technical and economic assessment of hybrid photovoltaic wind system with battery storage in Corsica Island, *Energy Policy*, 36 (2) (2008), pp. 743-754

Assessing the Profitability of New Investment Projects on Construction of Small HPP on HPS Crn Drim

Goce Bozinovski [1] and Atanas Iliev[2]

Abstract – **The Crn Drim basin is the richest with water from all of Macedonia. The paper gives the overview of the analyses made on practical example of the energy contribution and economical evaluation of the new planned hydro power plants of the cascade on hydro energy system of Crn Drim River in Macedonia. The existing hydro energy system consists of two cascade hydro power plants and three reservoirs, but the operation experiences and the site location give the possibility to upgrade the system with additional hydro power plants. The technical calculations and power improvement are the base platform to make the economical evaluation of the NPV, B/C, PBP values for each power plant from all over integrated hydro energy system. The geographical configuration of the terrain and hydrological conditions of the region, especially the tributaries of Radika river, allow construction of more hydropower plants. These hydro power plants would improve the energy situation in Macedonia, and also would regulate the operating mode of existing HPP.**

This paper will analyze more the hydropower projects in Crn Drim basin which are analyzed and planned for long time. The results presented in the paper are the energy production and economic viability of the construction and operation in power system.

Keywords – **Economy, Hydro Power Plant (HPP), Energy.**

I. INTRODUCTION

The main feature in the analysis of projects of hydroelectric plants is a high degree of uncertainty and imprecision of input parameters. Therefore, in order to perform an economic analysis of the projects, it is necessary to analyze multiple scenarios to determine the likelihood of certain option and meet investor risk investments of the HPP. As a challenge to show the many projects of hydroelectric determine those that are economically viable and feasible to consider those who the developer would guarantee the quickest return on investment. For this purpose will be determined and analyzed the financial performance of the planned investment of small hydropower on HS Black Drin.

The economic value of the power plants representing the following categories: NPV (Net Present Value), BCR (Benefit Cost Ratio), PBP, (Pay Back Period), IRR (Internal Rate of Return).

[1]Goce Bozinovski is with the AD ELEM-Skopje, Branch HES "Crn Drim"-Struga, Plostad na revolucijata bb, 6330 Struga, p.fax 83, R. Macedonia, e-mail: goce_boz@yahoo.com

[2]Atanas Iliev is with the Faculty of Electrical Engineering and Information Technologies – Skopje, Karpos II, 1000 Skopje, R. Macedonia,e-mail: ailiev@feit.ukim.edu.mk

II. BASIC PARAMETERS FOR THE SMALL HPP

This includes all projects of hydro power plants with installed capacity below 10 MW, which according to their projected energy parameters are treated as small hydropower plants with a reduced price of electricity in high tariff from 50 to 65 € / MWh and the low tariff of 45 € / MWh in correlation with preferential prices from Energy Regulatory Commission (ERC) of RM. In that group of potential small planned include: HPP Tresonce, HPP Gary, HPP Selce, HPP St. Petka and HPP Kosovrasti. These new hydropower plants are mostly tributaries of the supply to be used for filling the reservoir of potential HPP Boskov Most of Mala reka, and the existing reservoir of Debar Lake.

TABLE I
TECHNICAL PARAMETERS FOR THE PLANNED SMALL HPP ON HYDRO SISTEM CRN DRIM

	P_{inst}	W_{year}	CF– Capacity Factor	Economic analysis
	[MW]	[GWh]		
Tresonce	8	21	**0.30**	Indiv. project
Gari	2.7	9	**0.38**	Indiv. project
Selce	3.3	9	**0.31**	Indiv. project
Sv.Petka	1.2	4	**0.38**	Indiv. project
Kosovrasti	5.4	18	**0.38**	Indiv. project

Expected electricity production or capacity factor depends on annual production:

$$CF = \frac{W_{y\,ear}}{8760 \cdot P_{inst}} \quad (1)$$

Where is:

W_{year} - annual production of electricity,

P_{inst} - installed power units.

III. FINANCIAL INDICATORS FOR THE PLANNED SMALL HPP OF HS CRN DRIM

Small hydropower plants are have the following common input parameters: operation life of 20 - 25 years of the loan repayment of 10 years.The following table 2. presents an

overview of the economic indicators (NPV, B/C, CF, T_{kred}, T_{oper}, C_{ht} and C_{lt}) of the project analyzed the Small HPP hydro system Crn Drim. This presents economic indicators after all discounted benefits and costs. Where: T_{kred} - time of repayment of the loan in years; T_{oper} - operating life of the plant, number of years of operation for economic profit; C_{ht} - work in high tariff (peak load); C_{lt} - work in low tariff (base load).

Net Present Value (NPV) is obtained as:

$$NPV = NPV(B)_{1-n} - NPV(C)_{1-n} \qquad (2)$$

The B/C ratio is obtained as:

$$BCR = \frac{NPV(B)_{1-n}}{NPV(C)_{1-n}} \qquad (3)$$

Where is:

$NPV(B)_{1-n}$ - benefits for the whole operation life,

$NPV(C)_{1-n}$ - costs during HPP operation life.

TABLE II
ECONOMIC INDICATORS FOR PLANNED INVESTMENT PROJECTS OF SMALL HYDRO POWER PLANT ON CRN DRIM BASIN

HPP	NPV (€)	B/C	CF	T_{kred}_T_{oper} (year_year)	C_{ht}_C_{lt} (%_%)
Tresonce	2.316.40	1,21	0,30	10_25	60_40
Gari	2.435.79	1,33	0,38	10_20	60_40
Selce	1.217.89	1,33	0,38	10_20	60_40
Sv.Petka	465.89	1,10	0,31	10_20	60_40
Kosovrasti	792.99	1,45	0,38	10_20	50_50

On figure 1. and figure 2. presents graphical representations of economic indicators NPV and B/C for evaluation of new hydro power projects HPS Crn Drim.

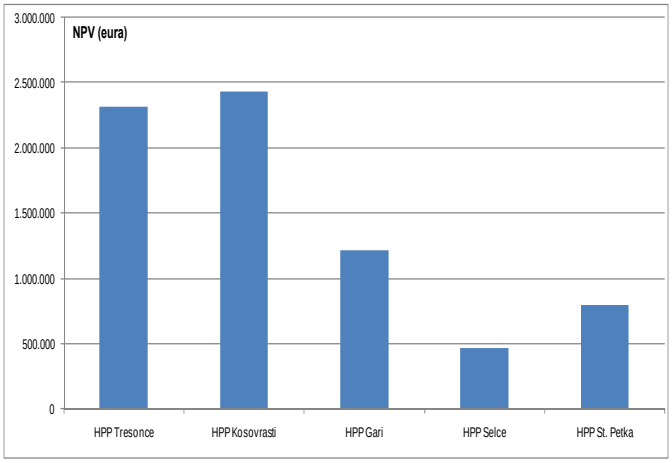

Fig. 1. NPV value for hydro projects on Crn Drim

The table and graphical presentation clearly show which projects are the most attractive for investors, as the group of small HPP, such as: HPP Gari, HPP Kosovrasti and HPP St. Petka. These plants have the highest factors of NPV and B/C> 1,3. Fig.3 shows the operational energy parameter of CF (capacity factor) for each hydro power plant which is directly connected to the economical indicators. CF is certainly linked to economic indicators, or those projects that have high economic indicators have high energy production with CF about 0,4. The peak load power plants have low CF which is about 0.3, such as: HPP Tresonce, HPP Selce.

The following figure 3. presented is a graphic indicator of exploitation CF for all hydropower projects analyzed, which is of course directly related to the the economic indicators for each project.

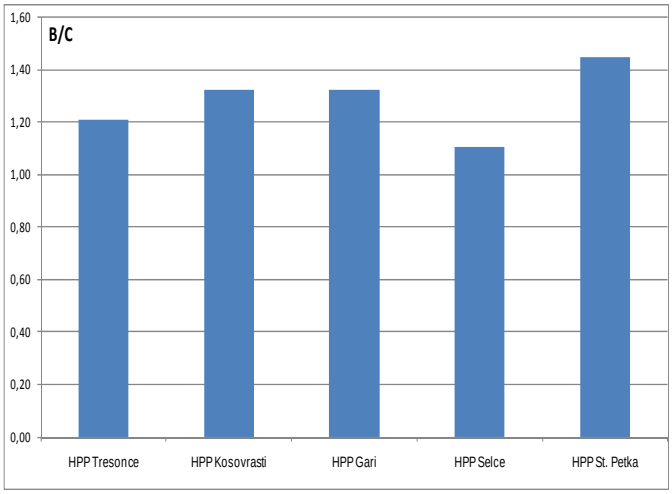

Fig. 2. B/C ratio for hydro projects on Crn Drim

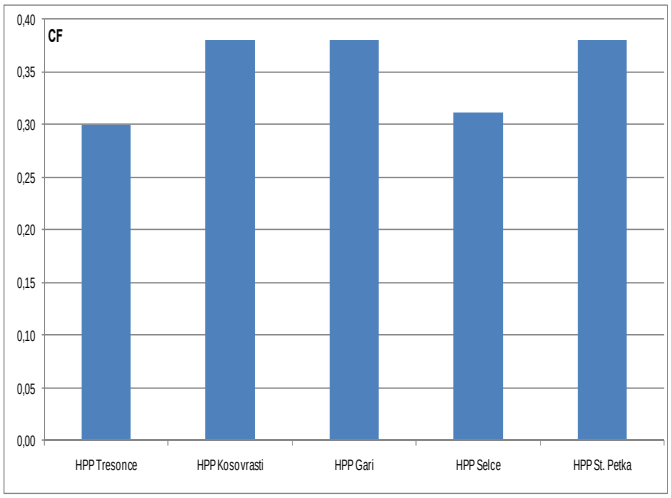

Fig. 3. CF for new small hydro projects on Crn Drim

Capacity factor CF gives the expected energy production wich is strongly connected with economic indicators. HPP Kosovrasti, HPP Gary and HPP Sveta Petka have CF value about 0.38 which is actually highly acceptable value. HPP Tresonce and HPP Selece have low CF which is

approximately below 0.3 which means that they have to operate in the peak load.

IV. Conclusion

The specific natural geographical position of the Crn Drim basin with all facilities (power plants, reservoirs and supply channels) plays an important role in the power system of Macedonia. With new hydro power facilities, the goal is to improve the energy value of the whole hydro system of Crn Drim as the followings:

- increased installed capacity,
- higher production of electricity,
- reduce spillovers,
- increased number of operation hours in peak load,
- reduced number of operational work as base load power plant.

Improving the energy value of hydropower production complex will certainly contribute to the financial benefit of the whole hydro complex. The main benefit of the system is the increased installed capacity and increased electricity production as well as reducing the spillover. Operating on the hydro power plants in the high tariff of peak load is particularly important in dry hydrology, and wet hydrological conditions can be avoided or minimized the overflows.

References

[1] Olsson, M., Söder. L.: "Hydropower Planning including Trade-off between Energy and Reserve Markets", Published in Proceedings of IEEE Bologna PowerTech 2003 June 23-26th Bologna Italy.

[2] Amir Pasha Zanjani Nasab; Financial Analysis of Small-Hydro Power Project in Malaysia from the Investor Perspective, 2012 IPCBEE Vol.33 (2012) Singapore.

[3] Technical documentation of hydro energy system of Crn Drim.

[4] Carmen L.T. Borges, Senior Member, IEEE, and Roberto J. Pinto: Small Hydro Power Plants Energy Availability Modeling for Generation Reliability Evaluation, IEEE, Vol 23, No.3 August 2008;

[5] G. Bozinovski, A. Iliev, "Energy Contribution and Economical Evaluation of Hydro Energy Complex System of Cascade Power Plants" – Renewable Energy Sources (OZE) 5th International Scientific Conference OZE 2014, High Tatras - Tatranske Matliare, May 20 – 22, 2014, Slovakia (467_OZE_2014, ISBN 978-80-89402-74-8).

This Page Intentionally Left Blank